Studies of angle-resolved photoelectron spectra from oriented NiCO: A model for adsorbed CO

Richard L. Dubs, Maile E. Smith,* and V. McKoy
Arthur Amos Noyes Laboratory of Chemical Physics, California Institute of Technology, Pasadena, California 91125
(Received 10 August 1987)

We present a study of angle-resolved photoelectron spectra from oriented, linear NiCO. We address the question: How well do simple cluster models such as oriented NiCO simulate adsorbate molecules with respect to photoemission? The photoemission cross sections are obtained using Hartree-Fock electronic continuum orbitals. For the bonding $5\bar{\sigma}$ orbital, we find oriented NiCO to be a better model than oriented CO. The large magnitude of the $5\bar{\sigma}$ photoionization cross sections relative to the $4\bar{\sigma}$ cross section cannot, however, be explained by our calculations without consideration of backscattering of the photoelectrons ejected "downward" into the detector.

I. INTRODUCTION

Angle-resolved photoelectron spectroscopy (ARPES) has evolved into a powerful probe of adsorbate-substrate interactions. This technique provides detailed information concerning both site geometry and electronic bonding character. For example, ARPES can help determine the orientation of adsorbed molecules and the orbital symmetries associated with photoelectron spectra.[1-3]

The prototype adsorbate-substrate system for ARPES studies has been CO on Ni.[4-12] Early continuum multiple-scattering calculations by Davenport[4] were helpful in establishing that, in most cases, CO bonds perpendicular to the Ni surface with the carbon end down. In these studies it was originally assumed that the only role of the surface was to orient the molecule, and ARPES from an oriented CO molecule was taken as a model for photoemission from adsorbed CO. For ARPES from orbitals not directly involved in bonding to the surface, e.g., 1π and 4σ, this approximation is a good one, and good qualitative agreement between theory and experiment is found for such cases.[5,8] However, as expected, oriented CO is a poor model for ARPES from orbitals directly involved in bonding to the metal surface, e.g., the 5σ orbital. A molecular fragment such as NiCO can be expected to be a more realistic model for photoemission from such orbitals. Recent studies have shown that local cluster models, e.g., NiCO, NiN_2, Ni_2CO, etc., can be good models for the chemisorption of N_2 and CO on Ni with regard to several spectroscopic properties.[13,14] Indeed, Davenport has studied the angle-resolved photoemission from the oriented, linear triatomic NiCO, again using the multiple-scattering method.[5]

The principle objective of the present studies is to answer the question, "How well do simple cluster models such as oriented NiCO simulate adsorbate molecules with respect to photoemission?" In an effort to assess NiCO as a model for CO adsorbed on Ni, we have carried out *ab initio* calculations of the ARPES spectra for NiCO as a function of energy. In these calculations, we use a Hartree-Fock wave function for the initial state of NiCO and frozen-core Hartree-Fock continuum orbitals in the final state. This method has been very successful in predicting and explaining a wide variety of phenomena relating to gas-phase molecular photoionization dynamics.[15] Our results indicate that oriented NiCO is a better model than oriented CO for the bonding 5σ orbital, while CO itself is adequate for the nonbonding, 4σ and 1π, orbitals. However, the magnitude of the measured 5σ photoemission cross section relative to that of the 4σ along the surface normal cannot be accounted for in our calculations without inclusion of backscattering of "downward" ejected photoelectrons into the detector.

II. METHOD

The cross section for photoionization of an initial bound state Ψ_i into a final state $\Psi_{f,\mathbf{k}}$ by linearly polarized light is proportional to the square of the dipole matrix element (in the length approximation)

$$I_{\mathbf{k},\hat{\mathbf{n}}}=k^{1/2}\langle\Psi_i\,|\,\mathbf{r}\cdot\hat{\mathbf{n}}\,|\,\Psi_{f,\mathbf{k}}^{(-)}\rangle\ , \tag{1}$$

where $\hat{\mathbf{n}}$ is the direction of polarization of the light and $\mathbf{k}$ is the momentum of the photoelectron. The doubly differential cross section in the molecular frame is then given by

$$\frac{d^2\sigma}{d\Omega_{\hat{\mathbf{k}}}d\Omega_{\hat{\mathbf{n}}}}=\frac{4\pi^2E}{c}\left|I_{\mathbf{k},\hat{\mathbf{n}}}\right|^2\ . \tag{2}$$

In these studies we use the Hartree-Fock wave function for Ψ_i in Eq. (1). For $\Psi_{f,\mathbf{k}}^{(-)}$ we invoke the frozen-core Hartree-Fock approximation in which the wave function is represented by an antisymmetrized product of $N-1$ bound orbitals, constrained to be identical to those of Ψ_i, and the photoelectron orbital. The determination of these photoelectron or continuum Hartree-Fock orbitals is a key step in the study of molecular photoionization.

In this approximation the photoelectron orbital satisfies the one-electron Schrödinger equation

$$[-\tfrac{1}{2}\nabla^2+V_{N-1}(\mathbf{r},R)-k^2/2]\Phi_{\mathbf{k}}(\mathbf{r},R)=0\ , \tag{3}$$

where V_{N-1} is the molecular ion potential at internuclear distance R, $k^2/2$ is the photoelectron kinetic energy, and $\Phi_{\mathbf{k}}$ satisfies the appropriate boundary condition. To obtain $\Phi_{\mathbf{k}}$ it is convenient to work with the integral form of Eq. (3), i.e.,

$$\Phi_{\mathbf{k}}=\Phi_{\mathbf{k}}^{c}+G_c^{(-)}V\Phi_{\mathbf{k}} , \tag{4}$$

where $\Phi_{\mathbf{k}}^{c}$ is the Coulomb scattering wave function, V is the molecular ion potential V_{N-1} with the Coulomb potential removed, i.e.,

$$V=V_{N-1}+\frac{1}{r} , \tag{5}$$

and $G_c^{(-)}$ is the Coulomb Green's function with incoming-wave boundary conditions, i.e.,

$$\left[-\tfrac{1}{2}\nabla^2-\frac{1}{r}-\frac{k^2}{2}\right]G_c(\mathbf{r},\mathbf{r}')=-\delta(\mathbf{r}-\mathbf{r}') . \tag{6}$$

Expansion of $\Phi_{\mathbf{k}}$ in a partial wave series about $\mathbf{k}$,

$$\Phi_{\mathbf{k}}(\mathbf{r})=\left[\frac{2}{\pi}\right]^{1/2}\sum_{l=0}^{l_p}\sum_{m=-l}^{l} i^l\Psi_{klm}(\mathbf{r})Y_{lm}^{*}(\hat{\mathbf{k}}) , \tag{7}$$

and substitution of this expansion in Eq. (4) shows that each Ψ_{klm} satisfies its own integral or Lippmann-Schwinger equation

$$\Psi_{klm}(\mathbf{r})=S_{klm}+G_c^{(-)}V\Psi_{klm} , \tag{8}$$

where S_{klm} is a partial wave Coulomb function. In Eq. (7) an infinite sum over l has been truncated at $l=l_p$.

To solve Eq. (8) we use two different methods both of which rely on separable approximations to a potential U of the form:

$$U(\mathbf{r},\mathbf{r}')=U^{s}(\mathbf{r},\mathbf{r}')=\sum_{i,j}\langle\mathbf{r}\mid U\mid\alpha_i\rangle(U^{-1})_{ij}\langle\alpha_j\mid U\mid\mathbf{r}'\rangle , \tag{9}$$

where the matrix $(U^{-1})_{ij}$ is the inverse of the matrix with elements $\langle\alpha_i\mid U\mid\alpha_j\rangle$. In one method, referred to as method A, the entire potential V of Eq. (4) is approximated by the separable expansion of Eq. (9). With this approximation the solutions of Eq. (8) are given by

$$\Psi_{klm}^{(0)}=S_{klm}(\mathbf{r})+\sum_{i,j}\langle\mathbf{r}\mid G_c^{(-)}V\mid\alpha_i\rangle(D^{-1})_{ij}\times\langle\alpha_j\mid V\mid S_{klm}\rangle , \tag{10}$$

where the matrix $(D^{-1})_{ij}$ is the inverse of the matrix with elements

$$D_{ij}=\langle\alpha_i\mid V-VG_c^{(-)}V\mid\alpha_j\rangle . \tag{11}$$

In the second method, referred to as method B, the potential V of Eq. (4) is broken into its direct and exchange components, V_{dir} and V_{ex}, respectively, the integral equation associated with V_{dir} is numerically integrated, and only the exchange potential is approximated by the separable expansion of Eq. (9). The full solution of Eq. (4) can then be readily obtained.[16] Since only the truly short-range exchange potential is approximated by Eq. (9), method B is particularly effective for obtaining solutions of Eq. (8) for the long-range potentials associated with strongly polar ions.

The basis functions $\alpha_i(\mathbf{r})$ in Eq. (9) can be chosen to be entirely discrete functions such as Cartesian Gaussian, spherical Gaussian, or Slater functions. In these studies we used a Cartesian Gaussian basis set centered on the nuclei. Such basis functions have been used successfully in electronic-structure calculations and are known to be effective in representing the multicenter nature of the scattering wave function in the near-molecular region. It is important to note that with only these discrete basis functions in the expansion of Eq. (9), the approximate scattering solutions $\Psi_{klm}^{(0)}$ of Eq. (10) do satisfy scattering boundary conditions. With adequate basis sets the continuum solutions $\Psi_{klm}^{(0)}$ can already provide quantitatively reliable and, at the Hartree-Fock level, variationally stable photoionization cross sections. In addition, we have developed iterative techniques for obtaining converged solutions of Eq. (8) and the associated cross sections.[16] Details of these iterative techniques and of the related numerical procedures which we have developed for solving these equations are discussed elsewhere.[16,17]

To obtain the ARPES spectra we expand the dipole matrix element of Eq. (2) in spherical harmonics

$$I_{\mathbf{k},\hat{\mathbf{n}}}=\left[\frac{4\pi}{3}\right]^{1/2}\sum_{l,m,\mu} I_{lm\mu}Y_{lm}^{*}(\hat{\mathbf{k}})Y_{1\mu}^{*}(\hat{\mathbf{n}}) , \tag{12}$$

where the dynamical coefficients $I_{lm\mu}$ are defined as

$$I_{lm\mu}=k^{1/2}\langle\Phi_i\mid r_\mu\mid\Psi_{klm}^{(-)}\rangle \tag{13}$$

for photoionization out of an orbital Φ_i and

$$r_\mu=\begin{cases}\mp(x\pm iy)/\sqrt{2} & \text{for } \mu=\pm1\\ z & \text{for } \mu=0.\end{cases} \tag{14}$$

In practice the summation over l in Eq. (12) is truncated at some $l=l_{\max}$. To obtain the differential cross sections of Eq. (2) we write $|I_{\mathbf{k},\hat{\mathbf{n}}}|^2$ as

$$|I_{\mathbf{k},\hat{\mathbf{n}}}|^2=\sum_{L'=0}^{2l_{\max}}\sum_{L=0}^{2}\sum_{M=-L}^{L}\beta_{L'LM}Y_{L'-M}(\theta_k,\phi_k)\times Y_{LM}(\theta_n,\phi_n) , \tag{15}$$

where

$$\beta_{L'LM}=[(2L+1)(2L'+1)]^{-1/2}\langle 1100\mid L0\rangle\sum_{l,m,\mu}\sum_{l',m',\mu'}(-1)^{m+\mu}[(2l+1)(2l'+1)]^{1/2}I_{lm\mu}I_{l'm'\mu'}^{*}\times\langle ll'00\mid L'0\rangle\langle ll'-mm'\mid L'-M\rangle\langle 11-\mu\mu'\mid LM\rangle . \tag{16}$$

Here (θ_k,ϕ_k) and (θ_n,ϕ_n) denote the polar angles for electron collection and photon polarization, respectively, in the molecular frame and $\langle l_1 l_2 m_1 m_2 \mid l_3 m_3 \rangle$ denotes a Clebsch-Gordan coefficient. The internuclear axis lies along the z axis of the molecular frame. In these studies we assume that the CO molecule is oriented along the laboratory frame z axis, i.e., normal to the Ni surface, and hence the laboratory and molecular frames coincide. Equations (15) and (16) can be easily modified for cases in which the two frames do not coincide. In general, for a given orientation of the molecule and photon energy, the $\beta_{L'LM}$ of Eq. (16) must be evaluated only once, after which Eq. (15) can be used to readily obtain the ARPES spectra for any experimental configuration of electron collection and photon polarization.

III. CALCULATIONS

For the self-consistent field (SCF) wave function of NiCO we used a contracted segmented $[3s,2p,1d]$ Cartesian Gaussian basis derived from a primitive $(9s,5p,1d)$ basis[18] on carbon and oxygen and an $[8s,6p,2d]$ set on the nickel contracted from a $(14s,11p,5d)$ basis.[19] This basis set was augmented with diffuse s and p functions with exponents of 0.1 and 0.05 at the center of charge of the CO bond. These basis functions with smaller exponents were added in between the carbon and oxygen nuclei so as to assure the correct behavior in the tail of the 5σ CO molecular orbital. Without such basis functions earlier studies[20] showed significant differences in the photoionization cross section obtained using identical continuum functions and a 5σ orbital expanded in a Slater basis or the standard valencelike Gaussian basis, e.g., $[4s,3p]$. Details of the CO calculations have been given previously.[20] We take the CO bond distance to be 2.173 a.u. and the Ni—C bond distance to be 3.477 a.u., which are the lengths of these bonds in $Ni(CO)_4$.[21] We also choose the ground electronic state of NiCO to be a $^1\Sigma^+$ state with a Ni $3d^{10}$ configuration. We assume this configuration for the Ni atom because this is its configuration in the ground state of $Ni(CO)_4$,[21] and, furthermore, studies of the electronic structure of both NiN_2 and NiCO showed their ground states to be $^1\Sigma^+$ and characterized by a significant Ni $3d^{10}$ component in the wave function.[13] With this choice, basis sets, and geometry, our SCF energy was -1618.7383 a.u.

The initial basis sets used in the solution of Eq. (8) for the photoelectron continuum orbitals of NiCO are shown in Table I. For these orbitals we used the procedure based on method B outlined above. The results presented here have not been iterated, since we found in previous work that iteration was often unnecessary in producing converged cross sections with method B. For the few checks we did perform, iteration showed no significant changes from the uniterated results. From

TABLE I. Gaussian basis sets used in obtaining the photoelectron orbitals for NiCO, defined as $\phi(r)=N(x-A_x)^l(y-A_y)^m(z-A_z)^n \exp(-\alpha \mid \mathbf{r}-\mathbf{A} \mid^2)$.

Center (A)	l	m	n	Exponent (α)
			$k\sigma$	
Ni	0	0	0	32.0, 16.0, 6.0, 2.0, 0.6, 0.2
	0	0	1	8.0, 2.0, 0.5
	0	0	2	2.0, 0.5
C	0	0	0	10.0, 4.0, 1.5, 0.5, 0.1
	0	0	1	1.0, 0.1
	0	0	2	1.0
O	0	0	0	10.0, 4.0, 1.5, 0.5, 0.1
	0	0	1	1.0, 0.1
	0	0	2	1.0
			$k\pi$	
Ni	1	0	0	32.0, 16.0, 6.0, 2.0, 0.6, 0.2
	1	0	1	8.0, 2.0, 0.5
C	1	0	0	10.0, 4.0, 1.5, 0.5, 0.1
	1	0	1	1.0, 0.1
O	1	0	0	10.0, 4.0, 1.5, 0.5, 0.1
	1	0	1	1.0, 0.1
			$k\delta$	
Ni	1	1	0	32.0, 16.0, 6.0, 2.0, 0.6, 0.2
C	1	1	0	10.0, 4.0, 1.5, 0.5, 0.1
O	1	1	0	10.0, 4.0, 1.5, 0.5, 0.1

our experience and such checks, the basis sets of Table I should provide reliable estimates of the photoionization cross section of NiCO. Several tests were also carried out to determine values of the truncation parameters of the partial wave expansions which would provide reasonably converged cross sections. As expected, our main concern here was the expansion parameters which would be adequate for the 1s orbital of the Ni atom. At the photoelectron kinetic energies in the studies, we found that the photoionization cross sections for the outer valence orbitals were insensitive to the actual convergence of the partial wave expansion of the 1s orbital. This, of course, assumes that the partial wave expansion of this orbital is scaled so that the orbital used in the numerical calculation is always renormalized to unity. Such a renormalization is also carried out for the other orbitals, including those for which the partial wave expansions are highly converged. For example, a partial wave expansion of $l_i^{\rm dir}=58$ for the orbitals in the direct potential of $NiCO^+$ led to essentially the same photoionization cross sections as using $l_i^{\rm dir}=29$, even though the normalizations for the 1σ orbital (essentially the 1s Ni orbital) were about 0.68 and 0.3, respectively.[20] In many of these calculations we consequently used the same choice of truncation parameters for the partial wave expansions as in our earlier studies of CO,[20] including $l_i^{\rm dir}=29$. However, several checks on the convergence of the associated cross sections were made by doubling the partial wave expansions. Such studies indicated that the cross section we present here are converged to within 5–10 %, which is appropriate for the present objectives.

All the cross sections presented here are obtained using the dipole-length approximation. As a check on the possible uncertainties in these cross sections arising from our use of approximate electronic wave functions, i.e., the Hartree-Fock form, we also obtained the cross sections in the dipole-velocity approximation. Although the cross sections obtained with the length and velocity forms do differ [e.g., in reference to Fig. 4, differential cross section (Mb/sr) for the $5\bar{\sigma}$ peak at $\theta_k=0°$ (length/velocity), 6.02/4.98; at $\theta_k=180°$, 9.10/7.38; for the $4\bar{\sigma}$ peak at $\theta_k=0°$, 6.75/6.40; at $\theta_k=180°$, 1.06/0.948], the conclusions we draw in this paper are independent of the actual form chosen.

The photon energies referred to in these studies assume the experimental values for the associated ionization potentials. For CO these are 19.7, 16.9, and 14.0 eV for the 4σ, 1π, and 5σ orbitals, respectively,[8] while for NiCO we use the experimental values for CO adsorbed on Ni, i.e., 16.5, 11.9, and 13.5 eV.[8] However, in comparing the spectra of CO and NiCO, we want to look at points in the spectra corresponding to the same photoelectron kinetic energy and not necessarily the same photon energy, since the former determines the photoelectron dynamics. Hence, in Figs. 1 and 3, the photoionization spectra for CO have been shifted down in photon energy by 3.2, 5.0, and 0.5 eV for the 4σ, 1π, and 5σ orbitals, respectively. Finally, although the 4σ, 1π, and 5σ levels of CO actually correspond to the 9σ, 3π, and 10σ orbitals in NiCO, in our discussion we will use the CO designations of $4\bar{\sigma}$, $1\bar{\pi}$, and $5\bar{\sigma}$.

IV. RESULTS AND DISCUSSIONS

In Figs. 1 and 2 we compare some of our calculated cross sections for CO and NiCO with the experimental data of Allyn *et al.*[7] for adsorbed CO. The CO is assumed oriented perpendicular to the Ni surface with the carbon end down. Here, and elsewhere, the angles (θ_i,ϕ_i) are standard polar angles where θ is measured relative to the z axis, $\phi=0°$ represents the positive x axis, and $\phi=90°$ the positive y axis. In these experiments[7] polarized light was used with $(\theta_i,\phi_i)=(45°,0°)$ and the photoelectrons were collected normal to the surface, i.e., $(\theta_k,\phi_k)=(0°,0°)$. The experimental data have been normalized by setting the peak value of the measured $4\bar{\sigma}$ photoemission cross section to the calculated $4\bar{\sigma}$ (NiCO) cross section. As expected, the "4σ" cross sections change little in shape and magnitude in going from CO to NiCO. Why the calculated $4\bar{\sigma}$ cross sections are shifted down from the experimental data will be discussed later. Recall, however that our calculated 4σ (CO) spectra are shifted down in energy by 3.2 eV for reasons discussed above.

Figures 1 and 2 also show that the calculated 5σ (CO) and $5\bar{\sigma}$ (NiCO) cross sections seriously underestimate the magnitude of the measured values. The NiCO results are only a slight improvement over those of CO. Although the experimental data also include contributions from photoionization of the $1\bar{\pi}$ level, its contribution is expected to be negligible for electron collection along the molecular axis.[22] Calculations confirm this behavior. Why then do the experimental results show the $5\bar{\sigma}$ cross section much larger than the $4\bar{\sigma}$ cross section while the calculations do not? This problem is especially disturbing for the NiCO case in which the bonding CO 5σ orbital should be fairly well described due to inclusion of the Ni atom. Of the many possible reasons

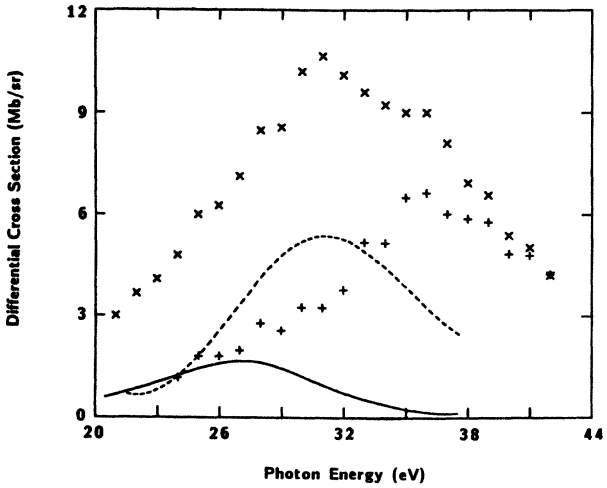

FIG. 1. Differential cross section vs photon energy for $(\theta_n,\phi_n)=(45°,0°)$ and $(\theta_k,\phi_k)=(0°,0°)$. Present results for CO: 4σ (– – –); 5σ (——). Experimental data of Allyn *et al.* (Ref. 7): $4\bar{\sigma}$ (+ + +); $5\bar{\sigma}+1\bar{\pi}$ (× × ×). See text for normalization of experimental data and energy scale for CO results.

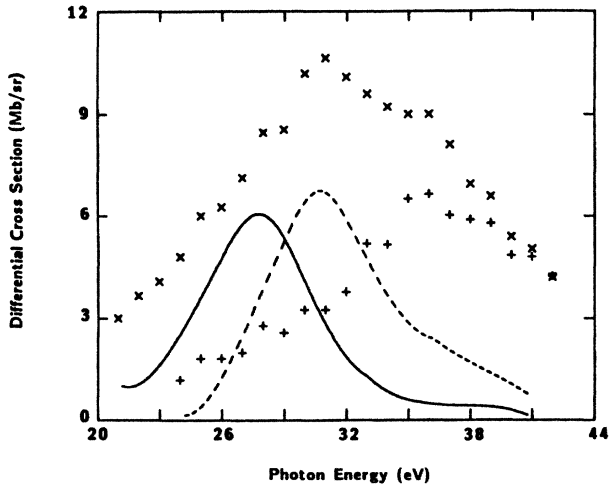

FIG. 2. Differential cross section vs photon energy for $(\theta_n,\phi_n)=(45°,0°)$ and $(\theta_k,\phi_k)=(0°,0°)$. Present results for NiCO: $4\bar{\sigma}$ (— — —); $5\bar{\sigma}$ (——). Experimental data of Allyn *et al.* (Ref. 7): $4\bar{\sigma}$ (+ + +); $5\bar{\sigma}+1\bar{\pi}$ (× × ×). See text for normalization of experimental data.

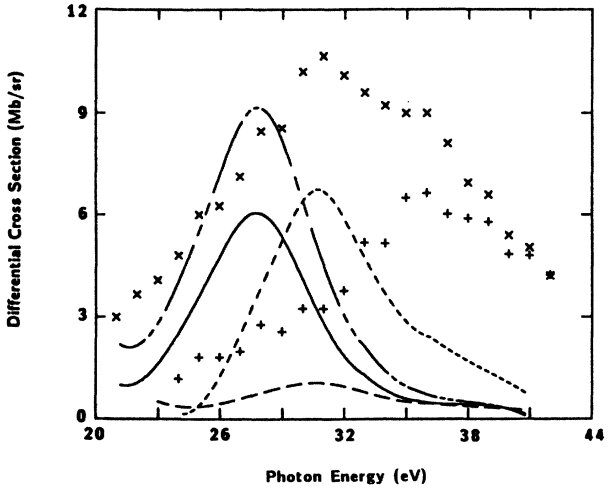

FIG. 4. See Fig. 2. Also shown are cross section at $(\theta_k,\phi_k)=(180°,0°)$ for NiCO: $4\bar{\sigma}$ (— — —); $5\bar{\sigma}$ (—··—).

for the significant differences between theory and experiment we have assessed two within the limits of our triatomic model. The first involves the Ni—C bond length used in our calculations. This distance, 3.477 a.u., is that found in $Ni(CO)_4$.[21] However, as noted by Kao and Messmer,[13] low-energy electron diffraction studies of CO adsorbed on Ni[100] suggest a bond distance of 3.25–3.40 a.u. For the s^0d^{10} configuration, Kao and Messmer[13] actually calculated a Ni—C bond length of 2.880 a.u. in NiCO, though they believe this value to be too short. To assess the influence of a shorter Ni—C bond distance on the $5\bar{\sigma}$ cross sections in NiCO, we repeated our calculations on NiCO with a Ni-C distance of 3.251 a.u. These results are not shown but retain the same qualitative features of Fig. 2.

Some insight into this discrepancy between theory and experiment could also be obtained by considering the

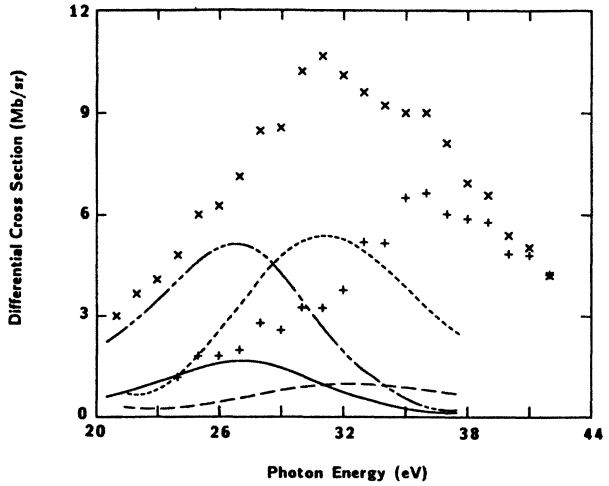

FIG. 3. See Fig. 1. Also shown are cross sections at $(\theta_k,\phi_k)=(180°,0°)$ for CO: 4σ (— — —); 5σ (—··—).

electrons photoejected downward from the adsorbed CO toward the surface. The theoretical results in Figs. 1 and 2 totally neglect these downward ejected electrons though, in reality, on an actual metal surface many of these electrons could be reflected back upward into the detector. In Figs. 3 and 4 we show the cross sections for these downward ejected electrons ($\theta_k=180°$) from CO and NiCO, respectively. For convenience, the results of Figs. 1 and 2 have also been included. Note that the cross section for downward ejected electrons from the "4σ" orbital or either CO or NiCO is negligible relative to the upward ($\theta_k=0°$) flux. This result is consistent with the fact that the 4σ orbital is localized on the oxygen end of CO and thus points away from the surface.

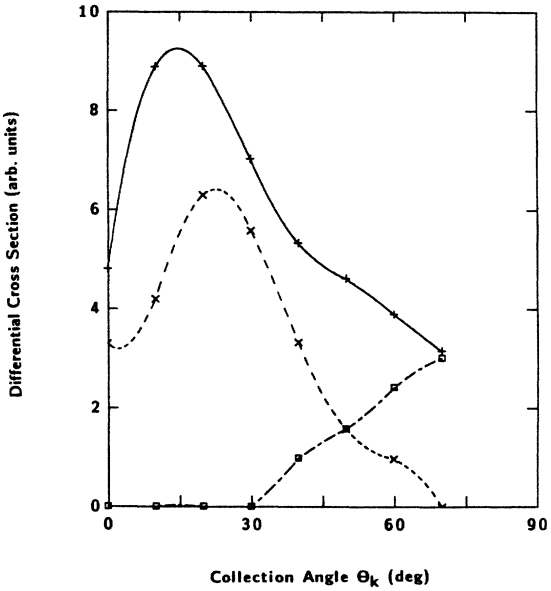

FIG. 5. Differential cross section vs the collection angle θ_k at $\phi_k=0°$ for unpolarized radiation. (See text.) Photon energy equals 40.8 eV. Experimental data of Williams *et al.* (Ref. 8): $5\bar{\sigma}$ (——); $4\bar{\sigma}$ (— — —); $1\bar{\pi}$ (—·—·—·).

However, the cross section for downward ejected electrons from the "5σ" orbital of CO or NiCO is *greater* than the upward cross section. This result is consistent with the fact that the 5σ orbital is located on the carbon end of CO and points directly toward the surface. Although with our simple NiCO model we cannot quantify the fraction of electrons reflected by the surface, our results suggest that these reflected electrons could be responsible for the large experimental $5\tilde{\sigma}$ cross section. Note that even if all the downward CO electrons in Fig. 3 were reflected upward into the detector along with the $\theta_k = 0$ electrons, our CO calculations would still not account for the large $5\tilde{\sigma}$ cross section. Our NiCO calculation of Fig. 4 is more suggestive in this respect.

In addition to predicting the incorrect magnitude of the $5\tilde{\sigma}$ peak in Fig. 2, the NiCO calculation does not account for the correct peak position or width. These latter discrepancies between the NiCO results and those of experiment are most likely due to relaxation effects.[7] As stated earlier, our studies used the frozen-core approximation, in which the orbitals of the ion are constrained to be identical to those of the neutral molecule. The frozen-core approximation used here completely neglects any screening of the molecular ion seen by the photoelectron.[22] Although this approximation may be appropriate for photoionization of gas-phase molecules, it can certainly be expected to work poorly for adsorbate

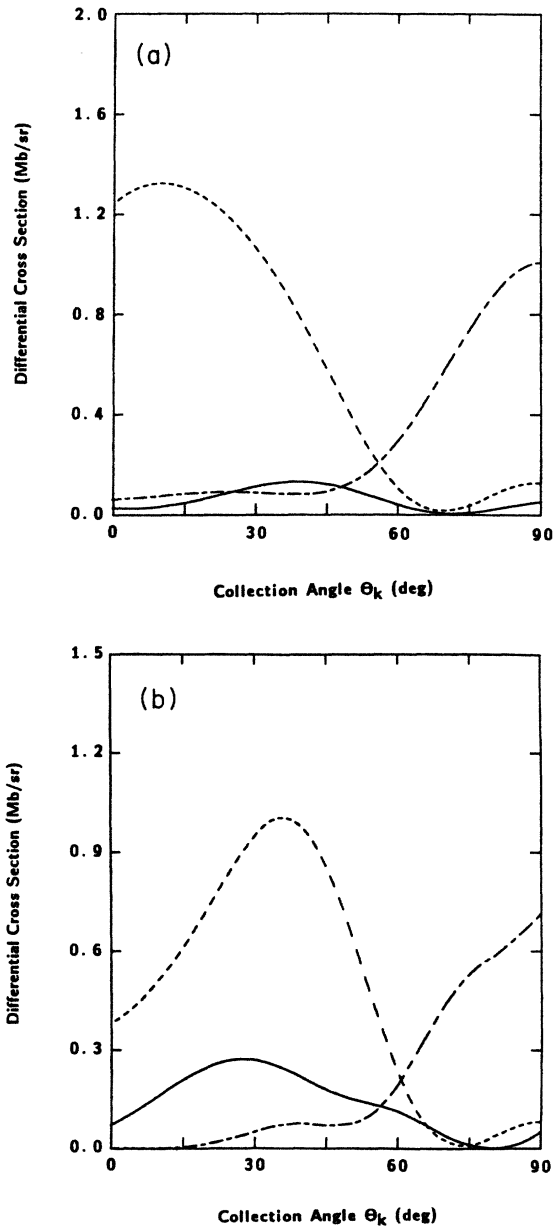

FIG. 6. Differential cross section vs the collection angle θ_k at $\phi_k = 0°$ for unpolarized radiation. (See text.) Photon energy equals 40.8 eV. 5σ (——); 4σ (— — —); 1π (—·—·—·). (a) Present results for CO; (b) present results for NiCO.

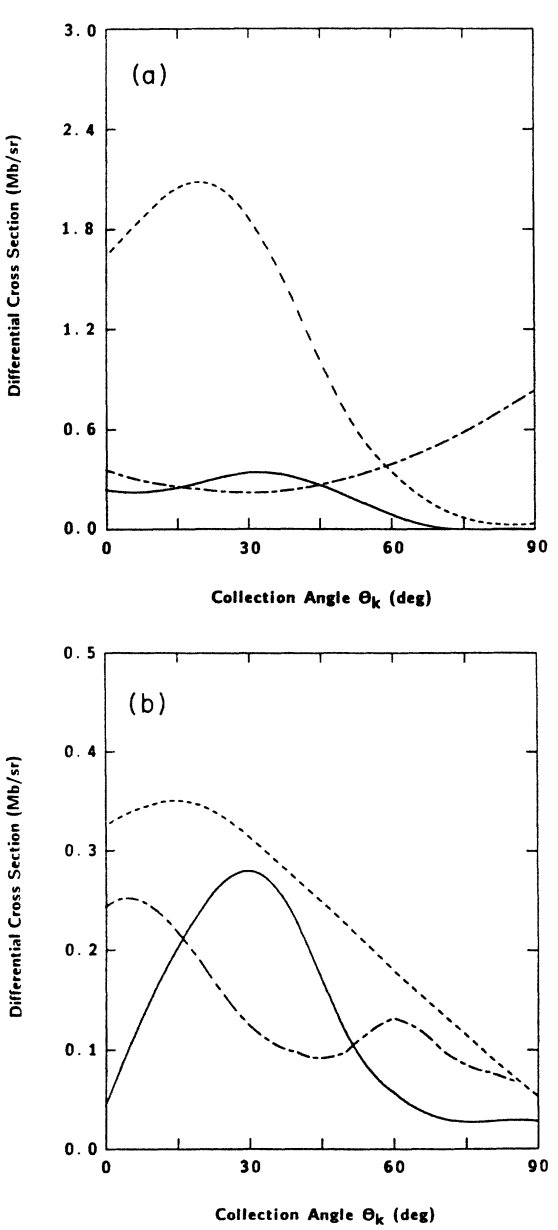

FIG. 7. Differential cross section vs the collection angle θ_k at $\phi_k = 0°$ for unpolarized radiation. (See text.) Photon energy equals 40.8 eV. 5σ (——); 4σ (— — —); 1π (—·—·—·). (a) Results of Ref. 5 for CO; (b) results of Ref. 5 for NiCO.

molecules on metals where electrons from the metal can very effectively screen and neutralize the adsorbate ion.

In addition to these energy-dependent studies, angle-resolved studies are an important test of our model for adsorbate photoemission. Figure 5 shows such data for CO on Ni[111].[8] In this experiment, unpolarized He II (40.8 eV) radiation was used, and the photon incidence angle was held fixed at 45° from the surface normal. Here we treat unpolarized light as two orthogonal linearly polarized components which contribute independently to photoemission.[10] One component is in the plane of incidence $(\theta_n,\phi_n)=(45°,0°)$ and the other is perpendicular to this plane, i.e., $(\theta_n,\phi_n)=(90°,90°)$. Photoelectron collection was in the incident plane $\phi_k=0°$. In Fig. 5 the emission intensities for the $4\tilde{\sigma}$, $1\tilde{\pi}$, and $5\tilde{\sigma}$ orbitals are shown as a function of the collection angle θ_k. These angular distributions agree qualitatively with the prediction by Grimley for photoemission from atomic p orbitals.[23]

In Figs. 6(a) and 6(b), our results for photoionization from oriented CO and NiCO, respectively, are shown. Our CO results have *not* been corrected for the difference in ionization potentials between gas-phase and adsorbed CO as was done in the energy-dependent studies shown in Figs. 1 and 3. This allows for a more-direct comparison with the multiple-scattering calculations of Davenport.[5] We do not consider surface-reflected electrons in these angular distributions since we cannot quantify this effect within our present model. Aside from an overall change of scale, our CO and NiCO results are very similar, with the $4\tilde{\sigma}$ peak shifted to slightly higher angles in the NiCO case. However, while the experimental results show the $5\tilde{\sigma}$ peak cross section greater in magnitude than that of the $4\tilde{\sigma}$ peak, both our CO and NiCO results show the $5\tilde{\sigma}$ peak far less in magnitude.

For comparison, Davenport's results[5] for photoionization from oriented CO and NiCO are shown in Figs. 7(a) and 7(b). Davenport's CO results are similar to our CO and NiCO results. His NiCO results, on the other hand, show some significant differences from those of CO. Aside from an overall change of scale, the $5\tilde{\sigma}$ peak has increased in magnitude relative to the $4\tilde{\sigma}$ peak, but, still in contrast to the experimental data, remains smaller. In addition, the NiCO $1\tilde{\pi}$ spectrum is very different from the CO results. Unfortunately, the experimental peak which Williams *et al.* assign as $1\tilde{\pi}$ might actually be substrate derived.[11]

As a final note, our model does not include the contribution from backscattering of downward ejected electrons by adjacent surface atoms. Similarly, we exclude the effects of photon reflection[24–26] and electron refraction[26] at the surface. These latter two contributions should not be very important in the experiments considered here. In all studies, the photon is incident at 45° from the surface normal, an angle at which reflection effects should be minimal,[24] especially at 40.8 eV where the angular studies are performed.[25] In the energy-dependent studies, collection is normal to the surface, where refraction effects should not be important.[27] We do not find refraction effects to be very important in the angular studies either (peaks are broadened and shifted to slightly higher angle),[27] and exclude them to make easier a direct comparison with the calculations of Davenport.[5]

In conclusion, we have performed *ab initio* calculations of angle-resolved photoelectron spectra from oriented, linear triatomic NiCO as a function of energy. For the orbitals not directly involved in bonding to the surface, we find that oriented CO provides a satisfactory model for CO adsorbed on Ni. However, for the $5\tilde{\sigma}$ orbital directly involved in bonding, oriented NiCO is better. The results of this cluster model cannot account for the large $5\tilde{\sigma}$ cross sections observed experimentally unless we consider the scattering of "downward" ejected photoelectrons into the detector. Our angular distributions for oriented CO agree reasonably well with those of the multiple-scattering model. However, our NiCO results do not.

ACKNOWLEDGMENTS

This work was supported by Grant No. CHE-85-21391 from the National Science Foundation. We also acknowledge use of the resources of the San Diego Supercomputer Center. One of us (R.L.D.) acknowledges support by the National Science Foundation.

*Present address: Institute for Defense Analyses, 1801 North Beauregard Street, Alexandria, VA 22311.

[1]E. W. Plummer and T. Gustafsson, Science **198**, 165 (1977).
[2]D. A. Shirley, J. Stöhr, P. S. Wehner, R. S. Williams, and G. Apai, Phys. Scr. **16**, 398 (1977).
[3]N. V. Smith, J. Phys. (Paris) Colloq. **39**, C4-161 (1978).
[4]J. W. Davenport, Phys. Rev. Lett. **36**, 945 (1976).
[5]J. W. Davenport, J. Vac. Sci. Technol. **15**, 433 (1978).
[6]S. Wallace, D. Dill, and J. L. Dehmer, Phys. Rev. B **17**, 2004 (1978).
[7]C. L. Allyn, T. Gustafsson, and E. W. Plummer, Chem. Phys. Lett. **47**, 127 (1977).
[8]P. M. Williams, P. Butcher, J. Wood, and K. Jacobi, Phys. Rev. B **14**, 3215 (1976).
[9]R. J. Smith, J. Anderson, and G. J. Lapeyre, Phys. Rev. Lett. **37**, 1081 (1976).
[10]G. P. Apai, P. S. Wehner, R. S. Williams, J. Stöhr, and D. A. Shirley, Phys. Rev. Lett. **37**, 1497 (1976).
[11]T. Gustafsson, Surf. Sci. **94**, 593 (1980).
[12]C. L. Allyn, T. Gustafsson, and E. W. Plummer, Solid State Commun. **28**, 85 (1978).
[13]C. M. Kao and R. P. Messmer, Phys. Rev. B **31**, 4835 (1985).
[14]H. J. Freund, R. P. Messmer, C. M. Kao, and E. W. Plummer, Phys. Rev. B **31**, 4848 (1985).
[15]See, for example, V. McKoy, T. A. Carlson, and R. R. Lucchese, J. Phys. Chem. **88**, 3188 (1984).
[16]M. E. Smith, R. R. Lucchese, and V. McKoy, Phys. Rev. A **29**, 1857 (1984).

[17]R. R. Lucchese, G. Raseev, and V. McKoy, Phys. Rev. A **25**, 2572 (1982).
[18]T. H. Dunning, Jr. and P. J. Hay, in *Modern Theoretical Chemistry 3,* edited by H. F. Schaefer III (Plenum, New York, 1977), p. 1.
[19]T. Smedley and W. A. Goddard III (unpublished).
[20]R. R. Lucchese and V. McKoy, Phys. Rev. A **28**, 1382 (1983).
[21]A. B. Rives and R. F. Fenske, J. Chem. Phys. **75**, 1293 (1981).
[22]D. L. Lynch and V. McKoy, Phys. Rev. A **30**, 1561 (1984); D. L. Lynch, Ph. D. thesis, California Institute of Technology, 1986.
[23]T. B. Grimley, Discuss. Faraday Soc. **58**, 7 (1974).
[24]S. P. Weeks and E. W. Plummer, Solid State Commun. **21**, 695 (1977).
[25]K. Jacobi, M. Scheffler, K. Kambe, and F. Forstmann, Solid State Commun. **22**, 17 (1977).
[26]M. Scheffler, K. Kambe, and F. Forstmann, Solid State Commun. **25**, 93 (1978).
[27]R. L. Dubs (unpublished).